Identification of the first Rho–GEF inhibitor, TRIPα, which targets the RhoA-specific GEF domain of Trio

Susanne Schmidt[a], Sylvie Diriong[a], Jean Méry[a], Eric Fabbrizio[b], Anne Debant[a,*]

[a] *CRBM-CNRS, UPR 1086 CNRS, 1919 Route de Mende, 34293 Montpellier Cedex 5, France*
[b] *IGM, UMR 5535 CNRS, 1919 Route de Mende, 34293 Montpellier Cedex 5, France*

Received 22 February 2002; revised 4 June 2002; accepted 4 June 2002

First published online 12 June 2002

Edited by Giulio Superti-Furga

Abstract The Rho–guanine nucleotide exchange factors (Rho–GEFs) remodel the actin cytoskeleton via their Rho–GTPase targets and affect numerous physiological processes such as transformation and cell motility. They are therefore attractive targets to design specific inhibitors that may have therapeutic applications. Trio contains two Rho–GEF domains, GEFD1 and GEFD2, which activate the Rac and RhoA pathways, respectively. Here we have used a genetic screen in yeast to select in vivo peptides coupled to thioredoxin, called aptamers, that could inhibit GEFD2 activity. One aptamer, TRIAPα (TRio Inhibitory APtamer), specifically blocks GEFD2-exchange activity on RhoA in vitro. The corresponding peptide sequence, TRIPα, inhibits TrioGEFD2-mediated activation of RhoA in intact cells and specifically reverts the neurite retraction phenotype induced by TrioGEFD2 in PC12 cells. Thus TRIPα is the first Rho–GEF inhibitor isolated so far, and represents an important step in the design of inhibitors for the expanding family of Rho–GEFs.

Key words: Exchange factor; Rho–GTPase; Trio; Peptide aptamer; PC12 cell

1. Introduction

Rho–GTPases are molecular switches that control actin cytoskeleton modifications during proliferation, transformation, cell migration and morphogenesis [1]. They cycle between an inactive, GDP-bound form and an active, GTP-bound form. Guanine nucleotide exchange factors (Rho–GEFs) accelerate GDP/GTP exchange, rendering the GTPase active [2]. Rho–GEFs share a conserved catalytic region termed the DH domain (for Dbl-homology) in reference to the oncogene *Dbl*, which was one of the first Rho–GEFs characterised [3]. A PH (Pleckstrin-homology) domain is always associated with the DH domain, suggesting that the DH–PH tandem is the functional unit in vivo. PH domains are thought to be involved mainly in subcellular localisation or in the regulation of DH-dependent exchange activity [4].

Trio is a complex protein containing two Rho–GEF domains of different specificity [5]. The first domain, TrioGEFD1, activates the Rac pathway via RhoG [6], and the second, TrioGEFD2, acts specifically on RhoA [5], indicating that Trio is able to link several Rho–GTPase pathways in vivo [7]. In addition, TrioGEFD1 binds to the actin-binding proteins Filamin and Tara, providing a direct link between Trio and the actin cytoskeleton [8,9]. Genetic studies of Trio homologues in *Caenorhabditis elegans* and *Drosophila* reveal that Trio plays a central role in neuronal cell migration and axon guidance [10–14] via a GEFD1-dependent process. The knock-out of the mouse Trio gene is lethal and Trio−/− embryos display defects in neuronal organisation and in muscle development [15]. Consistently, human Trio induces neurite outgrowth in PC12 cells and is involved in the nerve growth factor (NGF) pathway [16].

The large family of Rho–GEFs, like their GTPase targets, controls a variety of physiological processes, including transformation, metastasis, cell motility and neuronal development [17]. They are therefore attractive targets to design specific inhibitors that may have therapeutic applications. To identify such inhibitors, we utilised a recently developed genetic screen, allowing the in vivo selection of peptide aptamers that bind to a target protein and are thus potential inhibitors. Aptamers are short random peptides fused to the bacterial protein thioredoxin (Trx), which constrains them. Using TrioGEFD2 as a bait, we isolated one aptamer, TRIAPα (TRio Inhibitory APtamer), that specifically inhibited its in vitro exchange activity towards RhoA. The peptide sequence corresponding to TRIAPα, TRIPα (Trio Inhibitory Peptide), bound to TrioGEFD2 in mammalian cells and inhibited TrioGEFD2-mediated RhoA activation. In addition, TRIPα blocked TrioGEFD2 activity on neuronal morphology in PC12 cells but not that of the RhoA-specific GEF domain of the Trio-like protein Kalirin. In conclusion, this is the first report of a specific in vivo inhibitor of a Rho–GEF family member.

2. Materials and methods

2.1. Peptide aptamer screening and DNA methods

The TrioGEFD2 bait was constructed as follows: plasmid pMTHATrio5 was digested with *Eco*RI/*Xho*I and the insert (encompassing aa 1848–2298) cloned in pEG202 *Eco*RI/*Xho*I [18]. Yeast strain EGY048 [18] was transformed with this bait and subsequently with the library of Trx-constrained aptamers according to standard procedures. After transformation, cells were allowed to recover for 4 h in a galactose-containing medium before plating on a selective galactose medium. Of the 2×10^6 screened colonies, those growing in the absence of leucine were recovered and retested for interaction. Binding specificity was investigated by screening for interaction with other baits: TrioDH2 (aa 1848–2096), TrioPH2 (aa 2107–2223), Vav (aa 172–598), Dbl (aa 498–826) and Cdc2 [19].

The sequence of the variable moiety of the aptamer was determined using an ABIPRISM automated sequencer (Perkin Elmer). For GST

*Corresponding author. Fax: (33)-4-6752 1559.
E-mail address: debant@crbm.cnrs-mop.fr (A. Debant).

0014-5793/02/$22.00
PII: S0014-5793(02)02928-9

fusions, selected aptamers (including the *Trx* gene) were excised from pEG202 as *Eco*RI/*Not*I fragments and cloned into pGEX4T1 *Eco*RI/*Not*I. To create GFP–peptide fusion proteins, the variable region of the aptamers was amplified by polymerase chain reaction and cloned as an *Eco*RI/*Xho*I fragment into pEGFP-C3 *Eco*RI/*Sal*I.

2.2. Peptide synthesis

Peptide synthesis was performed on Fmoc-L-Met_PEG-PS resin (Applied Biosystems) as previously described [20]. The Fmoc deprotection time was increased all the synthesis long (7–9 min) and a 5 min capping by acetylation with 0.3 M acetyl imidazole in DMF was done after coupling to prevent deleterious peptide synthesis.

The peptide was deprotected, purified and analysed as described [20], except that dimethyl sulfide (3%) was added to the deprotection mixture to reduce methionine oxidation. FAB and MALDI mass spectra (MH+ = 4423) and amino acid analyses after HCl hydrolysis were in line with the expected structure.

2.3. In vitro GDP/GTP exchange assays

GTPase–GST fusion proteins were prepared, loaded with [^{3}H]GDP, and the guanine nucleotide release assay was performed as described [5], using recombinant GST–TrioGEFD2 (aa 1848–2298), TrioDH2 (aa 1848–2096), TrioGEFD1 (aa 1232–1629), Kalirin GEFD2 (aa 1850–2190), Dbl (aa 495–826), Lbc (aa 1–424) [22], p63RhoGEF (aa 149–374) and GST-tagged aptamers. For each point of the GDP-release assay, 0.3 μM GTPase was mixed with or without 0.4 μM GEF, and the reaction mix was filtered after 0 min and 15 min reactions at 25°C. The results are expressed as the ratio 'exchange after 15 min over exchange after 0 min' (% bound [^{3}H]GDP–RhoA).

The time course of [^{35}S]GTPγS binding was performed as described previously [21]. Briefly, 1 μM of GDP-loaded RhoA was mixed with or without 1.5 μM TrioGEFD2 in the presence of 10 μM [^{35}S]GTPγS at 25°C, and the reaction mix was filtered after the indicated times.

To measure the effect of the aptamers on the exchange activity, a 20-fold molar excess of GST-aptamer was pre-incubated with the GEFs for 30 min on ice before the exchange assays were carried out. For each experiment, data were obtained in triplicate.

2.4. Cell culture and transfection

COS-7 cells were maintained at 37°C in the presence of 5% CO_2 in Dulbecco's modified Eagle's medium supplemented with 10% foetal bovine serum. PC12–E2 cells were maintained and plated on collagen-coated 12 mm coverslips as described previously [16]. Transfection of PC12 and COS-7 cells was performed using Lipofectamine Plus (Life Technologies) according to the manufacturer's protocol.

2.5. RhoA activity assay

The level of GTP-bound form of RhoA was measured as described [23]. Briefly, COS cells were transfected with TrioGEFD2 in the absence or in the presence of GFP–TRIAPα. 48 h after transfection, cell lysates were subjected to GST pull-down, using the recombinant RBD fragment of the RhoA-specific effector Rhotekin. The presence of total RhoA and the GTP-bound form of RhoA in the samples was revealed on a Western blot using a monoclonal anti-RhoA antibody (Santa Cruz Biotechnology).

2.6. Immunofluorescence microscopy

After transfection and differentiation, PC12 cells were fixed and permeabilised as described [16]. Expression of proteins was visualised as indicated in the figure legend, and cells were observed under a DMR Leica microscope using a 40× planapochromat lens. Images were recorded using a Hamamatsu CCD camera. All transfections were repeated at least three times, and an average of 200 cells was counted each time. Cells with neurites are defined as cells with neurites of at least twice the length of the cell body.

3. Results

3.1. The aptamer TRIAPα inhibits the in vitro exchange activity of TrioGEFD2 towards RhoA

In order to identify specific inhibitors of TrioGEFD2, we used a recently developed strategy derived from the yeast two-hybrid system, where the cDNA library of preys has been replaced by a combinatorial library of short peptides (20 aa) in fusion with the bacterial protein Trx [18,24]. This strategy has been successfully used to isolate specific inhibitors of the cyclin-dependent kinases [18], the cell cycle transcription factor E2F [25] or the viral HPV16 E6 oncoprotein and HBV core protein [26,27]. Using TrioGEFD2 as a bait, 2×10^6 transformants were screened and, among the aptamers binding to TrioGEFD2 in yeast, three were selected for further analysis. These aptamers (TRIAPα, TRIAPβ, TRIAPγ) were tested against different baits as indicated in Fig. 1A: they interacted specifically with TrioGEFD2 and not with other Rho–GEF members such as Dbl and Vav, nor with a non-related protein such as Cdc2. TRIAPβ and TRIAPγ only bound to the DH2PH2 module, whereas TRIAPα also interacted with the DH2 catalytic domain.

The predicted amino acid sequence of the variable moiety of the aptamers is shown in Fig. 1B. These sequences showed no homology to each other nor to any sequence in the databases.

As described earlier, TrioGEFD2 displays specific exchange activity on RhoA [5] and not Rac or Cdc42. We next tested whether the TrioGEFD2-binding aptamers could inhibit the catalytic activity of TrioGEFD2 towards RhoA. For this purpose, the aptamers were expressed and purified from bacteria as GST fusion proteins and tested in an in vitro GEF assay, using recombinant TrioGEFD2 and RhoA proteins. The Rho–GEF activity was tested on [^{3}H]GDP-loaded RhoA in the presence of non-labelled GTP, where the catalytic activity of TrioGEFD2 was measured by the decrease of the GTPase-associated radioactivity. Preincubation (30 min) of a 20-fold molar excess of GST–TRIAPα with TrioGEFD2 significantly inhibited its in vitro catalytic activity towards RhoA, whereas the same amount of GST–TRIAPβ, GST–TRIAPγ or GST–Trx had no effect (Fig. 1C). The full inhibitory effect of TRIAPα on TrioGEFD2 catalytic activity was also obtained with only a 5-min-preincubation time, suggesting that the TRIAPα/GEFD2 complex had already reached an equilibrium (data not shown). In addition, GST–TRIAPα inhibited both TrioGEFD2 and TrioDH2 exchange activities, which is consistent with the fact that TRIAPα also recognised the DH2 catalytic domain in yeast.

3.2. Characterisation of the inhibitory effect of TRIAPα on TrioGEFD2 catalytic activity

To characterise the inhibitory effect of TRIAPα over time, we performed a time course of the GDP-release assay. TrioGEFD2 stimulated complete GDP-dissociation from RhoA within 20 min, whereas preincubation of GST–TRIAPα with TrioGEFD2 prevented the GDP-dissociation at any time points tested (Fig. 2A). To show that our GDP-dissociation assay reflected the GDP/GTP exchange, we also performed [^{35}S]GTPγS binding experiments on RhoA. As shown in Fig. 2B, GST–TRIAPα inhibited the [^{35}S]GTPγS binding on RhoA stimulated by GEFD2, while TRIAPβ had no effect. Moreover, inhibition of GEFD2 exchange activity by GST–TRIAPα was concentration-dependent, with an apparent half-inhibitory concentration of around 4 μM (Fig. 2C).

3.3. Specificity of TRIAPα inhibition

We next investigated whether TRIAPα inhibition was specific of TrioGEFD2 by testing the effect of GST–TRIAPα on other Rho–GEFs that display in vitro exchange activity on

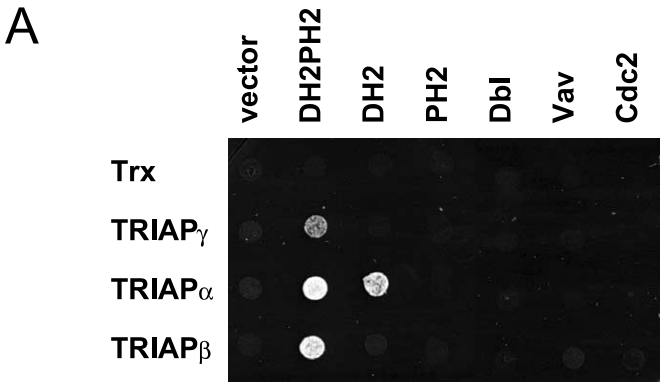

B

TRIAPα ASEGADGAICGYNLATLVMLGPSERVFCPLCEPCSSDIYELM
TRIAPβ IPKKYERSSPLRRPVRMMLR
TRIAPγ VLLREGRGFKVRLVVV

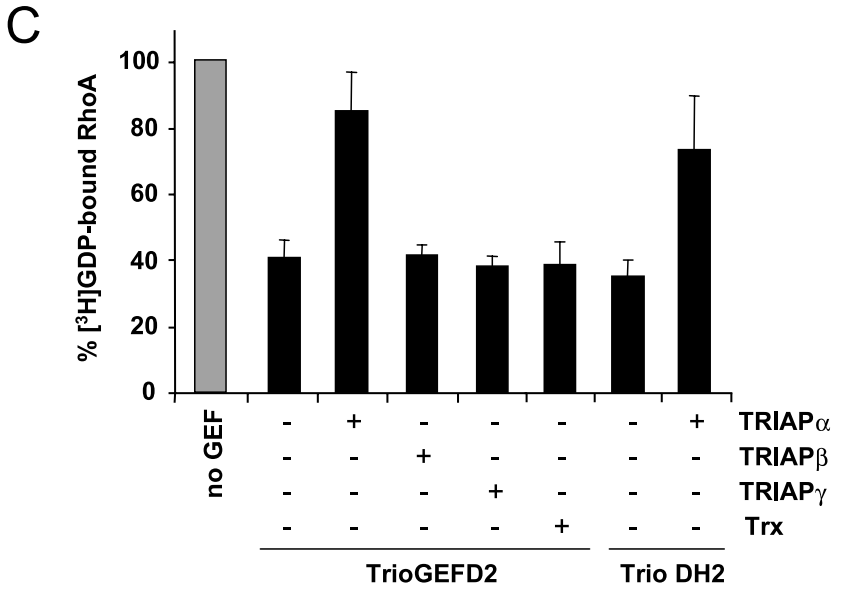

Fig. 1. TRIAPα inhibits TrioGEFD2-exchange activity on RhoA in vitro. A: Isolation of aptamers (TRIAPα, TRIAPβ, and TRIAPγ) binding to TrioGEFD2. The selected aptamers binding to TrioGEFD2 were tested for a specific interaction against different baits. Aptamers were co-transformed in yeast with either empty vector, Trio constructs (DH2PH2, DH2 or PH2), unrelated Rho–GEFs (Dbl, Vav) or Cdc2, and monitored for growth on a selective medium. Trx represents the Trx protein with no inserted peptide. B: Predicted amino acid sequence of the variable moiety of the selected aptamers. TRIAPα is a 42mer, TRIAPβ is a 20mer, whereas TRIAPγ is a 16mer. C: TRIAPα is a potent inhibitor of TrioGEFD2 activity. A 20-fold molar excess (8 μM) of GST aptamers TRIAPα, TRIAPβ, TRIAPγ or the empty Trx were pre-incubated 30 min at 4°C with 0.4 μM GST–GEFD2 or 0.4 μM GST–DH2, as indicated, before adding 0.3 μM of [^{3}H]GDP-loaded GST–RhoA. The exchange activity was monitored by the decrease of [^{3}H]GDP-bound RhoA after 15 min (see Section 2). The amount of [^{3}H]GDP-bound RhoA incubated without GEF was defined as 100%. The values and error bars are calculated from at least three independent experiments.

RhoA. We used different concentrations of Rho–GEFs to yield a similar nucleotide exchange efficiency, allowing us to compare the inhibitory effect of TRIAPα on the different GEF activities. The exchange activities of Lbc and Dbl (Fig. 2D and data not shown) were not affected by GST–TRIAPα. We then tested the effect of GST–TRIAPα on the catalytic activity of Rho–GEFs that display a high sequence similarity with TrioGEFD2: the recently identified RhoA-specific p63RhoGEF [28] (71.5% identity with TrioGEFD2) and the second Rho–GEF domain of the Trio family member Kalirin (KalGEFD2; 65% identity with TrioGEFD2). GST–TRIAPα had no effect on the catalytic activity of p63RhoGEF and

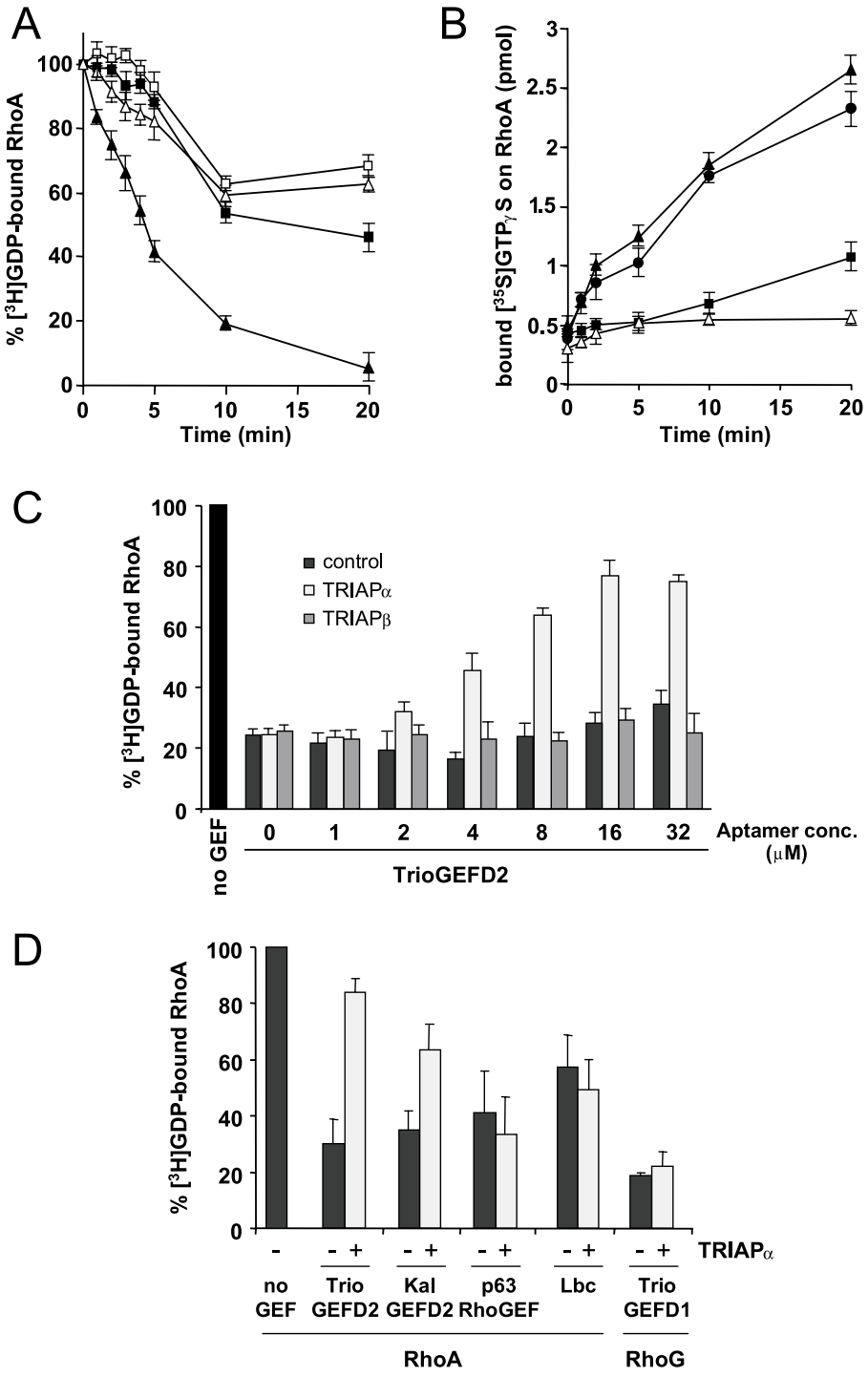

Fig. 2. Characterisation of the inhibitory effect of TRIAPα in vitro. A: Time of course of TrioGEFD2-induced guanine nucleotide release on RhoA after preincubation of TrioGEFD2 with GST–Trx (▲) or GST–TRIAPα (■). The spontaneous guanine nucleotide release on RhoA without TrioGEFD2 was measured in the presence of GST–Trx (△) or GST–TRIAPα (□). The exchange activity was monitored by the decrease of [^{3}H]GDP-bound RhoA at the indicated times as described in Fig. 1C. B: Kinetics of association of [^{35}S]GTPγS to GDP-loaded RhoA after preincubation of TrioGEFD2 with a 20-fold molar excess of GST–Trx (▲), GST–TRIAPα (■) or GST–TRIAPβ (●). △ represents the incubation of GDP-loaded RhoA with GST–Trx but not TrioGEFD2. C: TRIAPα inhibition of GEFD2 is dose-dependent. 0.4 μM GST–GEFD2 was incubated with increasing amounts of GST (black bars), GST–TRIAPα (light grey bars), or GST–TRIAPβ (dark grey bars), and the exchange assay was then performed on 0.3 μM RhoA as described in Fig. 1C. D: TRIAPα inhibition is specific of TrioGEFD2. To test the specificity of TRIAPα inhibition in vitro, exchange experiments were performed with different RhoA-specific GEFs: Trio GEFD2 (0.4 μM), Kalirin GEFD2 (KalGEFD2; 1.7 μM), p63RhoGEF (0.4 μM), Lbc (0.4 μM) and the RhoG-specific GEF domain of Trio (TrioGEFD1; 0.1 μM). Exchange assays were performed with the recombinant GEFs as described in Fig. 1C. We used different concentrations of Rho–GEFs to yield a similar nucleotide exchange efficiency. For each exchange factor, three independent experiments were done in the absence (black bar) or in the presence (light grey bar) of a 20-fold molar excess of TRIAPα.

A

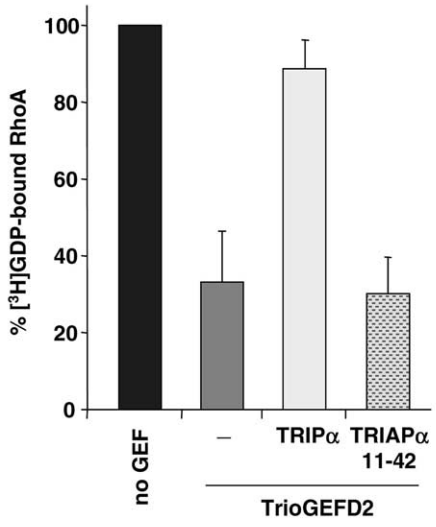

B

Amino acids	Sequence	Inhibition of TrioGEFD2 activity	
		TRIAPα	TRIPα
1 - 42	ASEGADGAICGYNLATLVMLGPSERVFCPLCEPCSSDIYELM	++	++
1 - 22	ASEGADGAICGYNLATLVMLGP	--	nd
22 - 42	PSERVFCPLCEPCSSDIYELM	--	nd
9 - 42	ICGYNLATLVMLGPSERVFCPLCEPCSSDIYELM	++	nd
11 - 42	GYNLATLVMLGPSERVFCPLCEPCSSDIYELM	--	nd
9 - 40	ICGYNLATLVMLGPSERVFCPLCEPCSSDIYE	++	nd
9 - 36	ICGYNLATLVMLGPSERVFCPLCEPCSS	++	--
9 - 33	ICGYNLATLVMLGPSERVFCPLCEP	+	--

Fig. 3. Characterisation of the TRIPα inhibitory properties. A: TRIPα shows the same inhibitory properties as TRIAPα. A 42-aa peptide corresponding to the variable moiety of TRIAPα, TRIPα, and a deletion of TRIAPα, TRIAPα 11–42, were tested in exchange assays for their ability to block TrioGEFD2 activity on RhoA. GEF assays were performed as described in Fig. 1C in the absence or in the presence of 8 μM of the different inhibitors, as indicated. B: Mapping of the minimal region of TRIAPα required for inhibition. Deletion mutants were created in the variable region of TRIAPα (still inserted in the Trx scaffold) or TRIPα, and tested for their ability to inhibit TrioGEFD2 activity in exchange assays (described in Fig. 1C). ++ represents the full retention of the inhibitory effect, while −− reflects the loss of inhibition. Nd signifies not determined.

partially inhibited KalGEFD2 exchange activity on RhoA. In addition, GST–TRIAPα did not block TrioGEFD1 activity on RhoG or Rac (Fig. 2Dand data not shown).

3.4. *TRIPα has the same inhibitory effect as TRIAPα*

TRIAPα blocked TrioGEFD2 exchange activity when its conformation was constrained by the presence of Trx. To evaluate the role of the Trx constraint in inhibition, we tested whether TrioGEFD2 activity could be blocked by a synthetic peptide of 42 aa, TRIPα, corresponding to the variable region of TRIAPα. At the same dosage (20-fold molar excess), TRIPα was as potent as TRIAPα in blocking the in vitro TrioGEFD2 exchange activity, suggesting that the Trx scaffold is not required for the TRIAPα inhibitory effect on TrioGEFD2 catalytic activity (compare Figs. 3A and 1C).

3.5. *Minimal TRIPα sequence requirements for inhibition of TrioGEFD2 exchange activity*

In order to map the sequence of TRIPα responsible for the inhibition of TrioGEFD2 activity, we tested different truncations of the TRIPα variable region on the inhibition of the in vitro TrioGEFD2 exchange activity (Fig. 3B). Deletion of the first eight amino acids of TRIAPα (TRIAPα 9–42) did not alter its inhibitory effect, while deletion of two additional amino acids (TRIAPα 11–42) completely abrogated its effect (Fig. 3A, B). Amino acids 9–36 displayed full inhibitory activity when constrained by the Trx scaffold, but not as a free peptide (TRIPα 9–36; Fig. 3B). These data suggested that the minimal sequence required for TrioGEFD2 inhibition is aa 9–36. However, in contrast to the full length TRIAPα, the TRIAPα 9–36 inhibitory effect was dependent on the presence of the scaffold.

3.6. *Inhibition by TRIPα of TrioGEFD2-mediated RhoA activation in intact cells*

We next wanted to determine the effect of TRIPα on GEFD2-mediated RhoA activation in intact cells. We first checked whether TRIPα could bind to TrioGEFD2 in mammalian cells. For that purpose, we designed vectors expressing the variable regions of TRIPα fused to GFP. GFP or GFP–

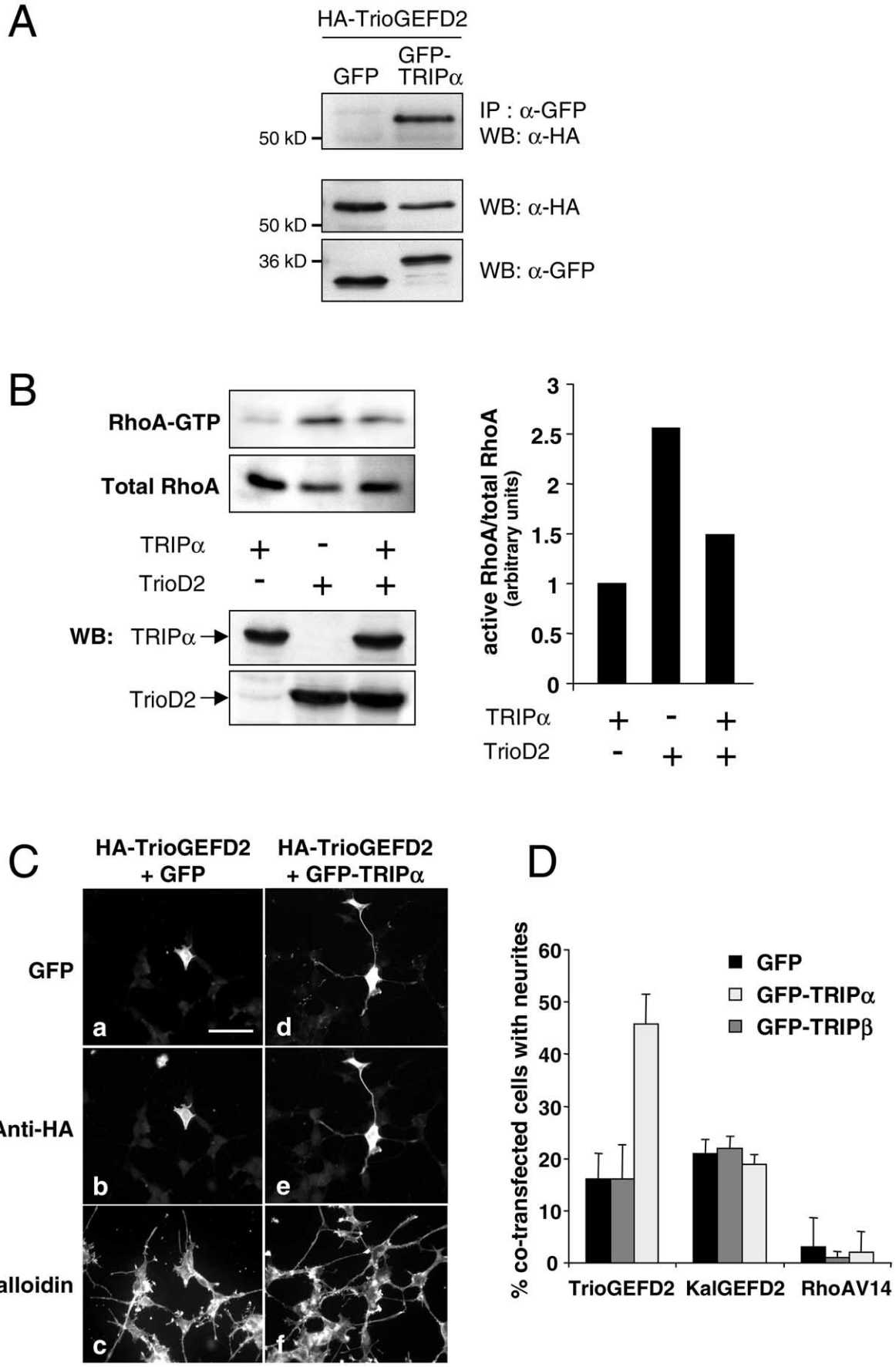
A
HA-TrioGEFD2
GFP
GFP-TRIPα
IP : α-GFP
WB: α-HA
50 kD
WB: α-HA
50 kD
36 kD
WB: α-GFP
B
RhoA-GTP
Total RhoA
TRIPα + - +
TrioD2 - + +
WB: TRIPα
TrioD2
active RhoA/total RhoA (arbitrary units)
3
2.5
2
1.5
1
0.5
0
TRIPα + - +
TrioD2 - + +
C
HA-TrioGEFD2 + GFP
HA-TrioGEFD2 + GFP-TRIPα
GFP
Anti-HA
Phalloidin
a
b
c
d
e
f
D
% co-transfected cells with neurites
60
50
40
30
20
10
0
GFP
GFP-TRIPα
GFP-TRIPβ
TrioGEFD2
KalGEFD2
RhoAV14

TRIPα were co-expressed with TrioGEFD2 in COS cells, and the protein interactions were studied by immunoprecipitation. TrioGEFD2 was present in the GFP–TRIPα-immunoprecipitates and not in the GFP-immunoprecipitates, indicating that TRIPα interacts with TrioGEFD2 in mammalian cells (Fig. 4A). We then wanted to assess the inhibition by TRIPα of TrioGEFD2-mediated activation of endogenous RhoA in intact cells. To do so, we made use of a GST fusion protein of the RhoA-specific effector Rhotekin (GST–RBD) in a pull-down assay from COS cell lysates to detect the active GTP-bound form of RhoA [23]. As shown in Fig. 4B, the activation of RhoA by TrioGEFD2 was significantly inhibited by the co-expression of GFP–TRIPα, showing that TRIPα is able to inhibit TrioGEFD2 activity in intact cells.

Numerous reports have established Rho–GTPases as key regulators of neuronal morphology [29]. In neuronal cell lines, activation of RhoG, Rac and Cdc42 induces neurite outgrowth, while RhoA stimulation antagonises this effect by promoting neurite retraction [30–32]. The PC12 cell line is a useful cellular model for studying NGF-induced neuronal differentiation. As already described in other studies [30], we observed that expression of an activated form of RhoA (RhoAV14) in PC12 cells prevented NGF-induced neurite outgrowth (Fig. 4D, black column). Similarly, we noticed that expression of TrioGEFD2 and KalGEFD2 also prevented NGF-induced neurite outgrowth, which is consistent with their specificity for RhoA. For example, only 16% of PC12 cells expressing HA–TrioGEFD2 extended neurites in response to NGF (Fig. 4D, black column), whereas more than 50% of cells usually respond to NGF treatment (data not shown). We then tested whether GFP–TRIPα could revert the inhibitory effect of TrioGEFD2 on NGF-induced neurite outgrowth. The expression of GFP–TRIPα alone had no effect on the NGF-differentiation signal (data not shown). Interestingly, co-expression of GFP–TRIPα with TrioGEFD2 reverted the Trio-dependent inhibition, since 45% of co-transfected cells extended neurites upon NGF treatment, while this reversion was not observed in presence of GFP alone or GFP–TRIPβ (Fig. 4C, D). Since TRIPα slightly inhibited KalGEFD2 exchange activity in vitro, we tested whether TRIPα was able to affect KalGEFD2 activity in vivo. In contrast to TrioGEFD2, neurite extension was similarly inhibited by KalGEFD2 either with or without GFP–TRIPα co-expression (Fig. 4D). Taken together, these data show that TRIPα specifically inhibits the effect of ectopically expressed TrioGEFD2 on PC12 cell morphology.

4. Discussion

In this study, we present the first isolation of a Rho–GEF inhibitor, TRIPα, specifically targeting the second Rho–GEF domain of the multifunctional protein Trio. This inhibitor binds to TrioGEFD2 in yeast and inhibits its in vitro catalytic activity towards RhoA. It does not significantly affect the activity of other RhoA-specific GEFs nor that of TrioGEFD1 towards RhoG, and thus seems to be specific for TrioGEFD2.

We show that the inhibition of the catalytic activity by TRIAPα is independent of the presence of the PH2 domain, since both GEFD2 and DH2 activities are affected. Given the fact that TRIAPα strongly interacts with TrioDH2 in yeast and that TRIAPα inhibition of TrioGEFD2 activity is dose-dependent ($IC_{50} = 4$ μM), we suspect that TRIAPα competitively inhibits the interaction of the DH2 domain with its GTPase target. It is noteworthy, however, that the TRIPα peptide sequence does not resemble any GTPase fragment that could prevent the interaction between TrioGEFD2 and its target. The mechanism of inhibition appears distinct from that proposed for the inhibition of ADP-ribosylation factor (Arf1) GTPase exchange factors by Brefeldin A [33]. Brefeldin A dramatically affects the structure of the Golgi apparatus by its capacity to stabilise an abortive ARF–GDP–GEF complex rather than preventing its formation. Thus, our inhibitor may represent the first example of a peptide acting as a competitive inhibitor between a GEF and its GTPase target.

In addition, TRIPα inhibition is not dependent on the Trx scaffold, suggesting that TRIPα adopts a functional three-dimensional structure on its own. Full inhibition can be achieved with TRIPα aa 9–36, but only when linked to the Trx scaffold. We propose that this 28-aa motif represents the active core for inhibition, while the flanking sequences stabilise its conformation. Characterising the molecular determinants underlying TRIPα inhibition of DH2-mediated catalysis will considerably aid our dissection of the mechanism of nucleotide exchange and specificity. Indeed, although the numerous members of the Rho–GEF family display distinct patterns of specificity for their GTPase targets, little is known about how this specificity is achieved at a molecular level.

Trio is the founding member of an emerging family of Rho–GEFs, including rat Kalirin, that possesses two GEF domains of distinct specificity. We found that TRIPα slightly inhibited the in vitro catalytic activity of Kalirin GEFD2. This is not surprising, considering the strong homology between the catalytic DH domains of Trio and Kalirin, espe-

←

Fig. 4. Inhibition by TRIPα of TrioGEFD2-mediated RhoA activation in intact cells. A: Interaction of HA–TrioGEFD2 with GFP–TRIPα in COS cells. HA–TrioGEFD2 was co-expressed with either GFP–TRIPα or GFP alone. The upper panel represents the immunoprecipitation with the anti-GFP antibody (IP: α-GFP) followed by a Western blot using the anti-HA antibody (WB: α-HA), and the lower panels represent the expression of the proteins in the cell lysates. B: Inhibitory effect of TRIPα on TrioGEFD2-mediated RhoA activation in intact cells using the RhoA activity assay. COS cells were transfected with TrioGEFD2, GFP–TRIPα or both. Cell lysates were subjected to GST pull-down using the recombinant RBD fragment of the RhoA-specific effector Rhotekin. The presence of the GTP-bound form of RhoA and of total RhoA protein was detected using a monoclonal anti-RhoA antibody and is represented in the upper two panels. GFP–TRIPα and TrioGEFD2 expression in the cell lysates is shown in the lower two panels. Quantification of the RhoA activity assay is shown in the right part of the figure. C: Inhibition by TRIPα of the TrioGEFD2 effect on neuronal morphology. Shown are immunofluorescence images of PC12 cells co-transfected with HA–TrioGEFD2 and either GFP–TRIPα (panels d–f) or GFP alone (panels a–c). After 48 h of expression, cells were treated for 16 h with NGF (50 ng/ml) and fixed. Expression of GFP and GFP–TRIPα was visualised directly (a, d), whereas overexpressed TrioGEFD2 was detected using the 12CA5 anti-HA antibody followed by AMCA-conjugated anti-mouse IgG (b, e). Filamentous actin was stained with Rhodamine-conjugated Phalloidin (c, f). Scale bar: 20 μm. D: Quantification of the TRIPα inhibition of TrioGEFD2-induced neuronal morphology. Cells were transfected with HA-tagged TrioGEFD2, myc-tagged KalGEFD2 or RhoAV14, and with either GFP–TRIPα, GFP–TRIPβ or GFP alone. Cells were processed as described in (C) and the number of co-expressing cells with neurites was counted. Note that only the TrioGEFD2 effect is reversed by TRIPα (light grey bar).

cially in the conserved regions CR1 and CR3 predicted to interact with the GTPase. Nevertheless, TRIPα efficiently interfered with the effect on neuronal morphology of TrioGEFD2 but not of Kalirin GEFD2, indicating TRIPα is functionally a very specific inhibitor of the RhoA-specific DH domain of Trio. Considering the fact that Trio and the brain-specific Kalirin have putative redundant functions in the nervous system, TRIPα thus represents a means to decipher their respective functions in this system.

Rho–GEFs such as Trio display several domains whose relative contribution to the function of the protein is not always understood. Developing aptamer inhibitors that target a precise domain represents an alternative inactivation strategy to the more classical knock-out techniques that target the activity or the expression of the entire gene product. We report here such an inhibitor that is a potent and specific inhibitor of TrioGEFD2 activity in living cells: (i) TRIPα coimmunoprecipitates with TrioGEFD2 and inhibits TrioGEFD2-mediated activation of RhoA in COS cells; (ii) TRIPα specifically inhibits the effect of ectopic TrioGEFD2 ectopic expression on neuronal morphology. It thus represents a powerful tool to determine precisely the role of TrioGEFD2, whose function in the context of the full length protein remains elusive.

Finally, this is the first report of a specific in vivo inhibitor of a Rho–GEF. Our peptide aptamer therefore represents an important step in the design of inhibitors specific for the expanding family of Rho–GEFs.

Acknowledgements: We thank Pierre Colas (ENS, Lyon, France) and Roger Brent (Molecular Sciences Institute, Berkeley, CA, USA) for kindly providing the aptamer library, Michael Olson (MRC, London, UK) for the kind gift of Dbl- and Vav- expressing plasmids, Deniz Toksoz (Tufts University, Boston, MA, USA) for the Lbc plasmid, Betty Eipper (John Hopkins University, Baltimore, MD, USA) for the Kalirin GEFD2 plasmid, and Pierre Travo, head of the CRBM Integrated Imaging Facility, for interest and support. Claude Sardet, Elodie Portales-Casamar, Soline Estrach and Philippe Fort are acknowledged for fruitful discussions, and Robert Hipskind and Philippe Pasero for critical reading of the manuscript. S.S. was supported by a fellowship from the Swiss National Science Foundation. This work was funded mainly by a grant from the Ligue Nationale contre le Cancer ('équipe labellisée') and by a grant from the Association pour la Recherche contre le Cancer (no. 5850).

References

[1] Hall, A. (1998) Science 279, 509–514.
[2] Boguski, M.S. and McCormick, F. (1993) Nature 366, 643–654.
[3] Hart, M.J., Eva, A., Zangrilli, D., Aaronson, S.A., Evans, T., Cerione, R.A. and Zheng, Y. (1994) J. Biol. Chem. 269, 62–65.
[4] Lemmon, M.A. and Ferguson, K.M. (2000) Biochem. J. 350, 1–18.
[5] Debant, A., Serra-Pages, C., Seipel, K., O'Brien, S., Tang, M., Park, S.H. and Streuli, M. (1996) Proc. Natl. Acad. Sci. USA 93, 5466–5471.
[6] Blangy, A., Vignal, E., Schmidt, S., Debant, A., Gauthier-Rouviere, C. and Fort, P. (2000) J. Cell Sci. 113, 729–739.
[7] Bellanger, J.M., Lazaro, J.B., Diriong, S., Fernandez, A., Lamb, N. and Debant, A. (1998) Oncogene 16, 147–152.
[8] Bellanger, J.M., Astier, C., Sardet, C., Ohta, Y., Stossel, T.P. and Debant, A. (2000) Nat. Cell Biol. 2, 888–892.
[9] Seipel, K., O'Brien, S.P., Iannotti, E., Medley, Q.G. and Streuli, M. (2001) J. Cell Sci. 114, 389–399.
[10] Steven, R. et al. (1998) Cell 92, 785–795.
[11] Bateman, J., Shu, H. and Van Vactor, D. (2000) Neuron 26, 93–106.
[12] Liebl, E.C. et al. (2000) Neuron 26, 107–118.
[13] Newsome, T.P., Schmidt, S., Dietzl, G., Keleman, K., Asling, B., Debant, A. and Dickson, B.J. (2000) Cell 101, 283–294.
[14] Awasaki, T., Saito, M., Sone, M., Suzuki, E., Sakai, R., Ito, K. and Hama, C. (2000) Neuron 26, 119–131.
[15] O'Brien, S.P., Seipel, K., Medley, Q.G., Bronson, R., Segal, R. and Streuli, M. (2000) Proc. Natl. Acad. Sci. USA 97, 12074–12078.
[16] Estrach, S., Schmidt, S., Diriong, S., Penna, A., Blangy, A., Fort, P. and Debant, A. (2002) Curr. Biol. 12, 307–312.
[17] Stam, J.C. and Collard, J.G. (1999) Prog. Mol. Subcell. Biol. 22, 51–83.
[18] Colas, P., Cohen, B., Jessen, T., Grishina, I., McCoy, J. and Brent, R. (1996) Nature 380, 548–550.
[19] Gyuris, J., Golemis, E., Chertkov, H. and Brent, R. (1993) Cell 75, 791–803.
[20] Morris, M.C., Mery, J., Heitz, A., Heitz, F. and Divita, G. (1999) J. Peptide Sci. 5, 263–271.
[21] Vignal, E., De Toledo, M., Comunale, F., Ladopoulou, A., Gauthier-Rouviere, C., Blangy, A. and Fort, P. (2000) J. Biol. Chem. 275, 36457–36464.
[22] Zheng, Y., Olson, M.F., Hall, A., Cerione, R.A. and Toksoz, D. (1995) J. Biol. Chem. 270, 9031–9034.
[23] Ren, X.D., Kiosses, W.B. and Schwartz, M.A. (1999) EMBO J. 18, 578–585.
[24] Geyer, C.R. and Brent, R. (2000) Methods Enzymol. 328, 171–208.
[25] Fabbrizio, E., Le Cam, L., Polanowska, J., Kaczorek, M., Lamb, N., Brent, R. and Sardet, C. (1999) Oncogene 18, 4357–4363.
[26] Butz, K., Denk, C., Ullmann, A., Scheffner, M. and Hoppe-Seyler, F. (2000) Proc. Natl. Acad. Sci. USA 97, 6693–6697.
[27] Butz, K., Denk, C., Fitscher, B., Crnkovic-Mertens, I., Ullmann, A., Schroder, C.H. and Hoppe-Seyler, F. (2001) Oncogene 20, 6579–6586.
[28] Souchet, M. et al. (2002) J. Cell. Science 115, 629–640.
[29] Luo, L. (2000) Nat. Rev. Neurosci. 1, 173–180.
[30] Kozma, R., Sarner, S., Ahmed, S. and Lim, L. (1997) Mol. Cell Biol. 17, 1201–1211.
[31] Katoh, H., Yasui, H., Yamaguchi, Y., Aoki, J., Fujita, H., Mori, K. and Negishi, M. (2000) Mol. Cell Biol. 20, 7378–7387.
[32] Yamaguchi, Y., Katoh, H., Yasui, H., Mori, K. and Negishi, M. (2001) J. Biol. Chem. 15, 15.
[33] Peyroche, A., Antonny, B., Robineau, S., Acker, J., Cherfils, J. and Jackson, C.L. (1999) Mol. Cell 3, 275–285.